Nature of Zeolite Distribution in the North Mountain Basalt, Southern Nova Scotia: Field and Geochemical Studies

D. J. Kontak

Introduction

Recent interest in the commercial development of zeolites in the Jurassic North Mountain Basalt (NMB) of the Annapolis Valley area, Nova Scotia, has focused attention on this world-class zeolite locality (Marshall, 1999). Although most world zeolite production is from altered tuffaceous rocks (pyroclastics), the abundance of zeolites in certain parts of the North Mountain Basalt has been recognized and the potential for a commercial zeolite industry in Nova Scotia may soon be realized. The dominant zeolite minerals in the NMB (Pe-Piper and Horton, 1996; Pe-Piper, 1997; and references therein) include types (e.g. heulandite, mordenite, stilbite) that have traditionally been mined and are commercially favored. In order to commercially develop any commodity, an adequate understanding of the distribution and properties of the commodity is a prerequisite. In fact, given that a considerable price difference exists for zeolite types, it is not only important to understand their distribution, but also the occurrence of each type. The present study focuses on addressing these important questions.

Although previous work on the distribution and types of zeolite within the North Mountain Basalt was recently summarized by Pe-Piper and Horton (1996), there is no detailed study of the actual distribution of zeolites within flows, nor a theory as to what controls this, although earlier observations (Hudgins, 1960; Aumento, 1962; and references therein) indicate that a zonal distribution occurs. Given that such information relates to potential development, this project focused on the distribution of zeolites within basalt flows. In order to determine what controlled zeolite distribution, outcrops of NMB were examined along the southern side of the Bay of Fundy from Scots Bay to Victoria Beach (Fig. 1). In addition, subsequent follow-up studies, including detailed petrographic and electron microprobe analysis, revealed new information regarding the nature of the zeolites, their distribution within the basalts, mineral paragenesis, and processes responsible for zeolite formation. In this paper, initial results on the distribution of zeolites and their genesis are presented. Studies pertaining to the thermal conditions of formation and nature of the mineralizing fluids are continuing and will be reported on at a later time.

Field Relationships and Observations

The North Mountain Basalt (ca. 10,000 km^2; Colwell, 1980; Greenough and Papezik, 1987) was deposited ca. 202 Ma (Hodych and Dunning, 1992) in the Bay of Fundy graben and forms part of an extensive Mesozoic basalt province along eastern North America. Basalts of similar age and composition along this basalt province were also deposited in small rift basins in response to lithospheric extension accompanying opening of the Atlantic Ocean. The NMB, which forms a prominent topographic high along the northern margin of the Annapolis Valley, dips northwestward (3-10°) and varies from ca. 400 m thick at Digby to ca. 275 m thick near Cape Split. Basalt, part of the Fundy Group, is underlain by continental red conglomerate and sandstone (Wolfville Formation) and siltstone and shale (Blomidon Formation). Unconformably overlying the basalt are lacustrine limestone, calcareous sandstone and time equivalent continental clastic rocks (Scots Bay Formation).

The internal stratigraphy of the North Mountain Basalt, as described by Papezik *et al.* (1988), consists of three main units (but note that Colwell, 1980, gives a slightly different description): (1) a lower, massive flow, 190 m thick at Digby to 50 m thick near Cape Split, which is medium- to coarse-grained; (2) a middle unit, up to 50 m thick, composed of a series of thin amygdaloidal lavas; and (3) an upper, massive unit of phenocryst-rich basalt which is about 160 m thick near Digby. On the north shore of the Bay of Fundy four thin flows totalling 74 m comprise a fourth unit which underlies the basal unit (1) mentioned above (Greenough *et al.*, 1989).

The North Mountain Basalt was examined at several localities along the coastline and inland (Fig. 1), but given the excellent exposure along the coast most of the data collected came from such localities. At the coastal

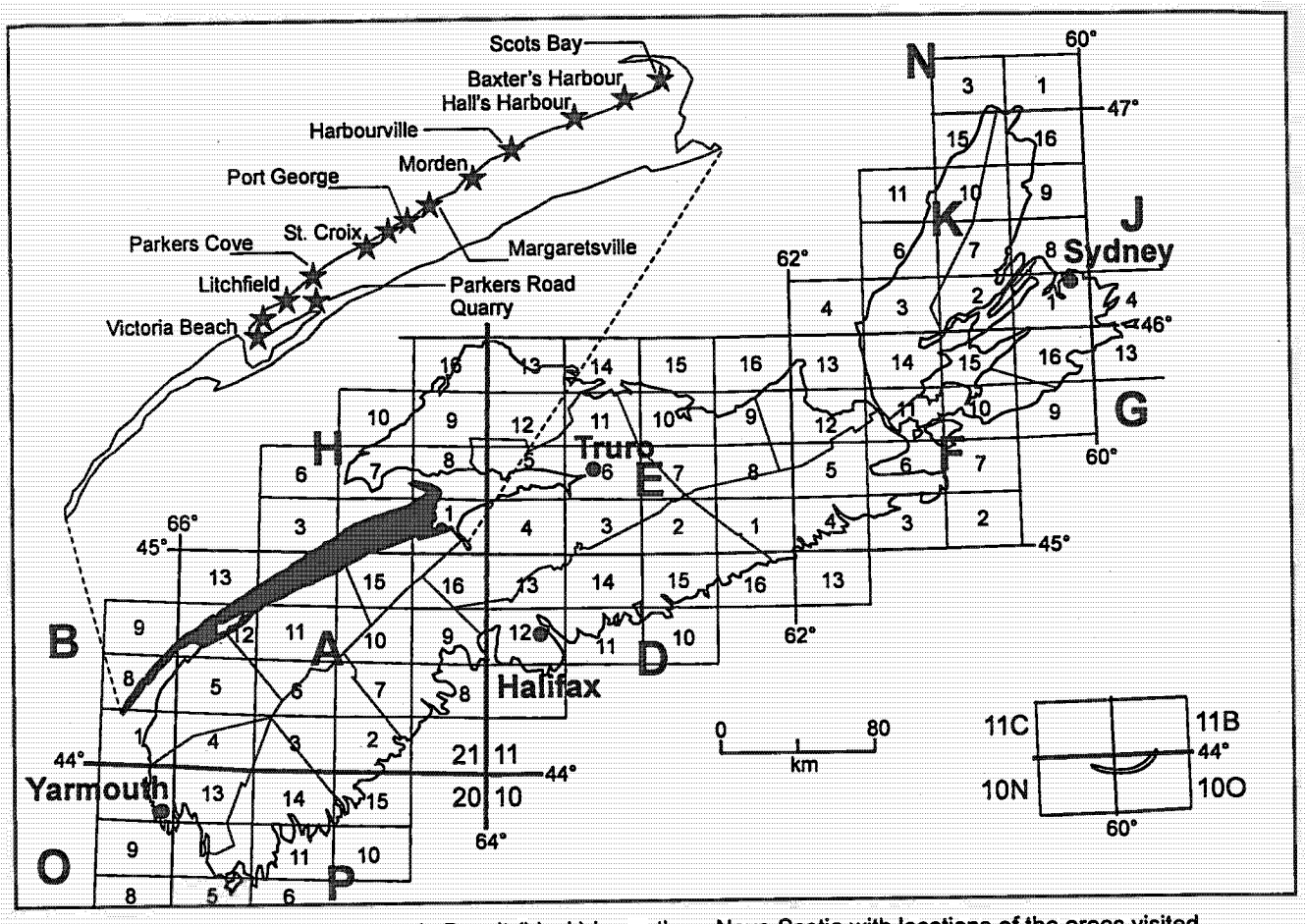

Figure 1. Outline of the North Mountain Basalt (black) in southern Nova Scotia with locations of the areas visited.

stops, traverses of several kilometres were made and particular note was taken of the number of flows and the distribution of zeolites both vertically and laterally. Despite the limited vertical and lateral continuity of inland outcrop, the features of the basalt are similar to those examined along the coast, thus similar conclusions are made.

Individual flows observed are generally ca. 8-10 m thick (rarely to ca. 20 m) and this is uniform for considerable distances where flows could be followed along coastal sections; the exception to this was noted at the Parker Cove quarry near Annapolis Royal where a single flow >100 m thick is exposed. Flows generally have a flat to slightly inclined dip, indicating a flat paleotopography during volcanic activity in the areas examined. The contact zones between flows are sharp, but rare cases of irregular surfaces have been observed, including 1-2 m depressions or gullies and corrugated tops (Fig. 2). A distinct reddening occurs in the top 1-2 m of some flows (Fig. 2d), which is presumed to relate to oxidation.

The flows are variable in their texture with massive, isotropic flows the most common. The basalt is generally dark grey-green and fine grained with plagioclase laths and an ophitic texture visible in the coarser-grained parts of flows. Within a flow the texture is uniform, except with notable chilling seen towards flow bottoms. The only additional textures observed were amygdules; there were no xenoliths, pegmatites, interflow sediments or felsic lenses, features that have been observed elsewhere in the North Mountain by previous workers (e.g. Greenough and Dostal, 1992b, c; C. White, personal communication, 1999).

Fractures (flat, vertical and circular) are locally common and these features are described here because of their importance in providing porosity and permeability in the basalt for zeolite formation. Flat fractures may occur randomly throughout a flow (Fig. 2e) or dominate the upper half, with fracture density progressively increasing toward flow tops (Fig. 2c, d). The interval between fractures is commonly 10-20 cm and fractures rarely continue for more than a few

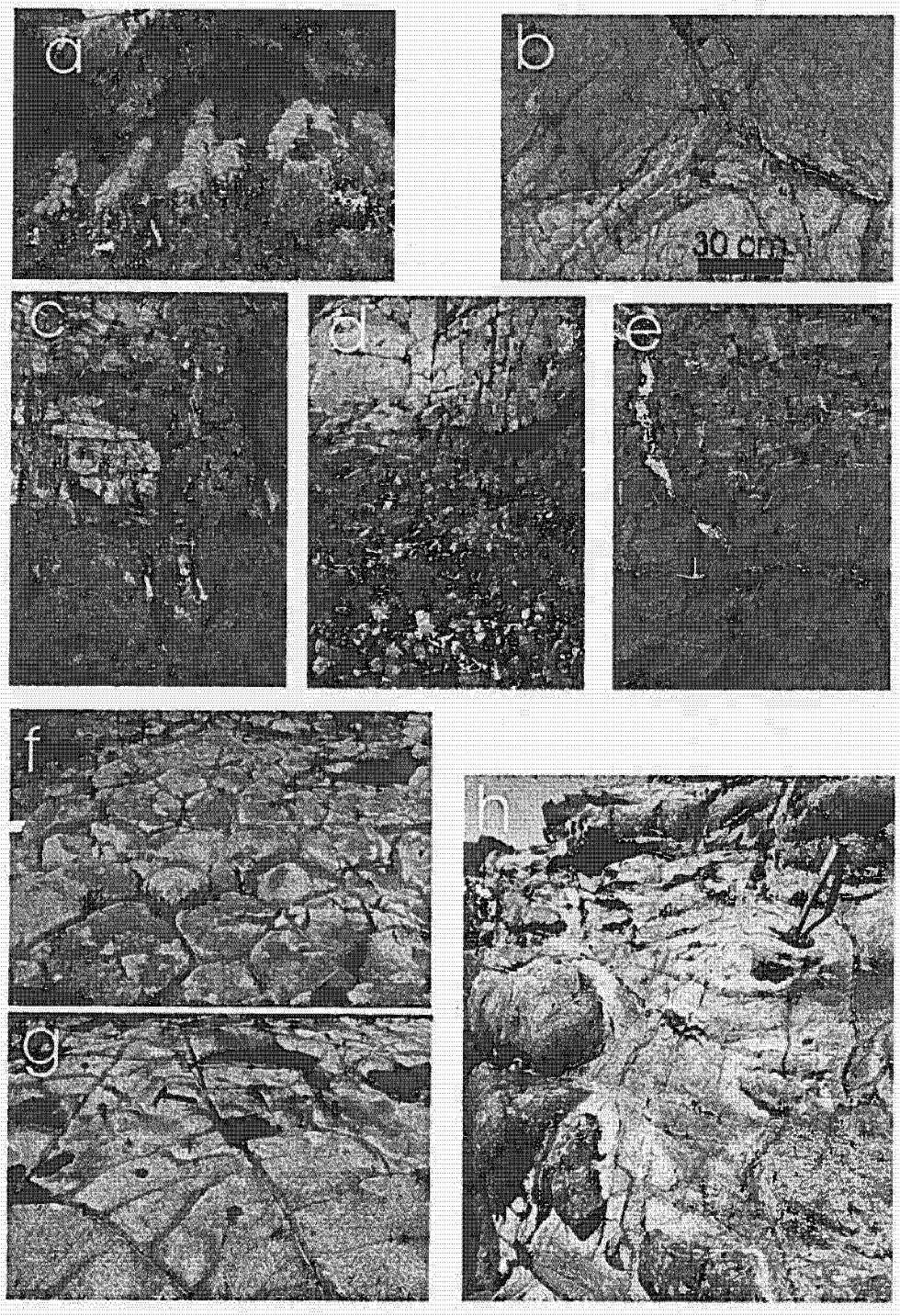

Figure 2. Field photographs of North Mountain Basalt. (a) Corrugated top of a flow beneath another flow at St. Croix Cove. This texture is similar to ropy tops of pahoehoe flows. (b) Contact between two massive flows with well-developed planar fracturing in the upper part of the lower flow. (c) Two flows of basalt showing well-developed planar fracturing. Note the very regular spacing (ca. 0.5 m) developed in the upper flow and more irregular density of fracturing in the lower flow. (d) Irregular fracturing in basalt flow with remnant areas of massive texture (no fractures) preserved. (e) Columnar jointing in basalts along the coast at Port George. (f) Columnar jointing in basalt with incipient alteration along the joints. Note the circle around hammer for scale. (g) Close-up of triple junction in columnar jointed basalt showing alteration along the joints and later infill by fine-grained silica. Knife is shown for scale. (h) Large-scale development of spheroidal weathering in basalt.

metres before coalescing with other fractures (Fig. 2e). One of the most conspicuous and common structural features is the development of vertical columnar jointing (Fig. 2f), best observed between Margaretsville and Litchfield in what may be the same flow. The scale of the joints is exceptionally consistent with columns having a width of ca. 1 m. Locally, alteration along the columnar joints imparts a positive relief and enhances the columnar pattern (Fig. 2f). Alteration zones are also developed parallel to these fractures and often vein silica infills fractures (Fig. 2g; also see below). Vertical fractures, in a generally N-S orientation, also occur and these fractures may traverse an entire flow.

Spheroidal weathering is a common feature of areas where well-developed fractures occur. This weathering creates areas of basalt dominated by a bulbous shape with diameters of ca. 0.5 to 1 m. This feature may be mistaken as being a pillow-like structure, but lacks the typical interconnecting concave-convex patterns and tear-drop bottom structures that characterize pillow basalts. The spheroidal weathering is merely a manifestation of preferential weathering along intersecting fracture patterns, in this case flat (horizontal) and vertical fractures that are locally developed in the basalt (Fig. 2h). Hudgins (1960) came to a similar conclusion regarding these features.

The basalt has been subjected to two distinct, but temporally and spatially related, hydrothermal events that deposited zeolite minerals and silica. Whereas the zeolite minerals occur along most of the coastal area, except for very sparse development between Port George and Litchfield, silica veins are best developed east of Baxters Harbour (Fig. 1), where mutually cross-cutting relationships with zeolites are observed.

Zeolite Distribution and Classification

Based on field observations along the coastal section and a few inland exposures, a four-part classification is proposed for the occurrence of zeolites. The purpose of this classification is two-fold: first to provide a predictive means of delineating and following zeolite-rich zones for use by industry, and second to explain the occurrence of such zones by a model. Classification of the zones, summarized from field observations in Figure 3, consists (from bottom to top) of the following characteristics.

(1) The basal zone (Fig. 3a, b) contains rare disseminated amygdules, occluded and empty, and elongate vesicles (10-20 cm) occluded most often with zeolites, but rarely with a green phase (mica). Amygdules in this zone rapidly diminish vertically and, in fact, are really only concentrated in the bottom 20-30 cm of flows. In addition, there is a general trend for coarser amygdules to occur at the top of this zone, perhaps reflecting coalescence of bubbles (see below). The elongate amygdules occur at the top of the disseminated amygdule zone and are generally, but not always, inclined at 40-50°. In a single locality these elongate amygdules had a sigmoidal shape, similar to sigmoidal shear veins, and a sinistral sense of movement. The elongate amygdules have a flat, downward-facing side and an irregular, upward-facing side, and adjacent amygdules may be connected. The basal zone is overlain by up to a few metres of massive, non-vesiculated basalt.

(2) The bubble-train zone (Fig. 3c, d, e) displays extreme lateral continuity and consists of vertical (ca. 1 m), cigar-shaped pipes ca. 10-20 cm in diameter within which are zeolite-bearing amygdules. Hudgins (1960) observed these pipes infilled with agate and other silicate minerals in addition to zeolites. The amygdules, about 1-2 cm in diameter and irregular to subrounded in shape, constitute ca. 10-25 volume % of the pipe and there appears to be no obvious variation in the diameter or shape of amygdules within pipes. The maximum thickness of this zone is 4 m and the distance between pipe cores is generally uniform for a given area at 0.4 to 0.7 m. Minor amounts of flat, sheet-like zones of zeolite-bearing amygdules occur within the bubble train zone. These sheets are not seen to cut the pipes, but this relationship is not well constrained given the rarity of the sheets.

(3) The upper part of the bubble-train zone coalesces into a laterally continuous zone of inter-connected vertical pipes and flat, amygdule-rich zones which is referred to as a net-textured zone (Fig. 3f). Massive basalt lies between the amygdule-rich pipes and flat zones, and is generally, but not always, void of vesicles. This zone is ca. 1-2 m thick where present.

(4) The top of the flows contains a laterally continuous, massive disseminated zone of 1-2 m thickness which consistently contains the highest amount of amygdules, locally 25-30% (Fig. 3g, h). Zeolite-bearing amygdules are both uniformly disseminated and also aligned along flat, planar features or sheets. The amygdules in this zone are generally <1-2 cm long, but some are 10-20 cm.

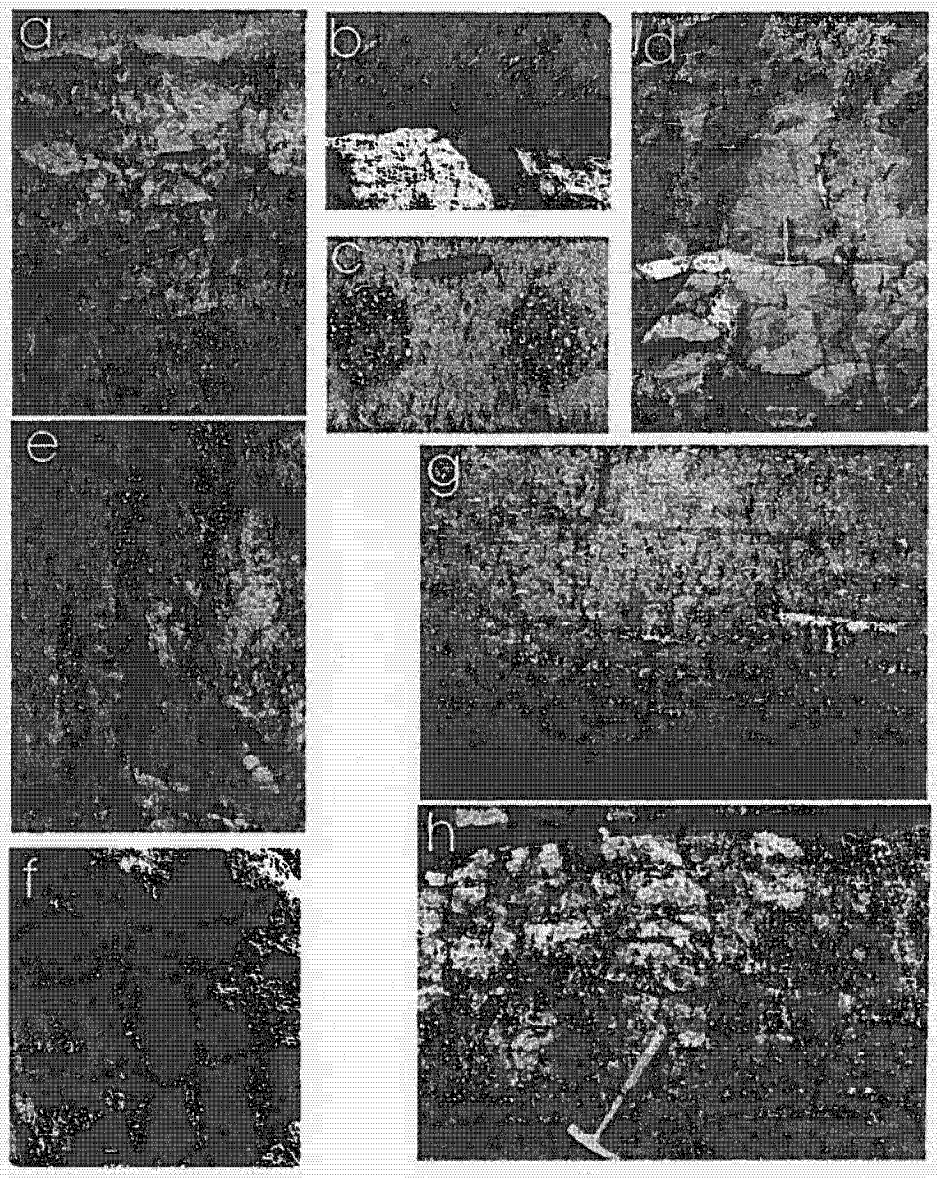

Figure 3. Field photographs of amygdules infilled with zeolites in North Mountain Basalt. (a) Two basalt flows with lower flow dark from red, hematitic alteration and also containing ca. 10% zeolites. The bottom of the overlying flow is characterized by two types of amygdules: (1) elongate, cigar-shaped amygdules that are uniformly inclined at 45-50° and occur ca. 20 cm from the bottom of the flow, and (2) small, equant amygdules that are most abundant at the base of the flow and quickly diminish upwards. In this particular occurrence only about 50% of the vesicles are infilled with zeolite. (b) Close-up of the base of a basalt flow showing in detail the shape of the elongate amygdules that characterize the basal zone. Note that the similar inclination of the amygdules, their concentration within one zone, and their uniform spacing and length. (c) Plane view of bubble-train zone showing the spherical shape of the pipes as defined by the area of amygdules. Note the absence of similar size vesicles or amygdules in the surrounding massive basalt. (d) Basalt flow of ca. 6 m thickness with very well developed bubble-train zone with pipes ca. 0.5 to 1.5 m in length. Note the massive, amygdule-free zone beneath the bubble-train zone. Note how this zone merges into the net-textured zone at the top of the photo. (e) Close-up of a bubble-train zone showing the pipe shape of the amygdule-rich areas and the very consistent length:width ratio of the pipes. (f) Net-textured zone of amygdules where the bubble-train zone has merged with a laterally extensive zone of amygdules resulting in a continuous network of amygdaloidal basalt with intervening massive, amygdule-free basalt. (g, h) Upper zone of massive disseminated amygdules where zeolites are most abundant. Note in Figure 3g that the zeolites define thin, laterally continuous sheet zones with intervening areas free of amygdules, whereas in Figure 3h areas of vesicular basalt without infill of zeolites are preserved between zeolite-rich zones.

Petrography of Zeolites and Basalts

Petrographic study of massive and amygdaloidal basalt was done with a transmitted light microscope and imaging facilities attached to the electron microprobe at Dalhousie University (Fig. 4). In transmitted light, fresh basalt specimens reveal euhedral clinopyroxene and plagioclase as isolated crystals and part of glomeroclasts, equant to skeletal Fe-Ti oxides and a dark brown mesostasis, considered to be late-stage glass that is variably crystallized. Examination of the mesostasis material in reflected light indicates an abundance of fine-grained skeletal oxide phases with textures identical to those described by Philpotts (1978, 1979, 1982) as representing crystallized Fe-rich melt formed from late-stage liquid immiscibility in tholeiitic basalt. Imaging of this same mesostasis material indicates a range of textures (Fig. 4c, d, e, g) that are considered to represent crystallization of immiscible felsic and mafic liquids under a range of cooling conditions (cf. Philpotts, ibid., and references therein). Where plagioclase and pyroxene are in contact with the mesostasis material (Fig. 4c, e, f), syntaxial overgrows of markedly different composition occur.

Altered basalt, that is amygdaloidal basalt with zeolite and other phases occluding the porosity, varies considerably in the modal proportions of minerals. Minerals present, in addition to those in fresh basalt, are mainly zeolites, albite and various mica phases, K-feldspar, Fe-oxides, and alkali amphibole, as summarized in the BSE images and mineral paragenesis figures (Figs. 5 and 6). Pe-Piper (1997) also notes the presence of barite rosettes, gypsum, and Au, Cu and Ni minerals lining pores in the zeolites (Fig. 6). The fact that zeolite and mica occur as alternating layers within the amygdules indicates fluctuations in the conditions responsible for mineral deposition. A common feature noted in this study is the albitization of plagioclase with later replacement by zeolite (Fig. 5a, b, d) and then minor amounts of K-feldspar cross-cutting the albite (Fig. 5d, e). Within the matrix of basalt occurs an abundance of zeolites as a replacment of fine-grained feldspar, replacing mesostasis material or infilling very irregular-shaped vesicles (Fig. 5f). The complexity of the paragenesis is well represented by the relationship between zeolites and micas; for example, the variation in relative timing of these two phases is shown in Figures 5c, g, i and k. The complexity of the mica textures and mineralogy is illustrated in Figures 5g and h, where the fibrous nature of this mineral phase is shown. Early formation of Fe-oxide phases, pre-dating zeolite mineralization, is documented in Figure 5j.

Finally, the most interesting feature of all is shown in Figure 5l where early K-feldspar rimming a vesicle is seen to be cross-cut by later alkali amphibole (riebeckite).

Geochemistry

Geochemical analyses of the basalt and amygdule mineralogy were done at Dalhousie University using a JEOL 733 Superprobe equipped with an energy dispersive system. Operating conditions were 15 kV accelerating voltage, 15 nA beam current, 1-10 μm beam diameter and a 40 second counting time for point analysis. In addition, rastering analyses were done in order to obtain chemical analysis of basalt and the intergranular matrix; in such cases the areas rastered varied depending on the situation.

Raster Analysis of Matrix

Raster analysis on two types of basalt matrix material is summarized in the ternary plots shown in Figures 7 and 8. The areas rastered correspond to the intergranular matrix (IM) between phenocrystic phases (i.e. plagioclase and pyroxene) and a late mesostasis material (MM) which was originally glass (i.e. intergranular to the matrix phases). Note that in the chemical data are compared to whole-rock analysis of fresh North Mountain Basalt from Greenough and Dostal (1992a). With respect to the analytical results (Figs. 7 and 8), the following points are noted. (1) In general, the IM deviates markedly from the MM, with a notable enrichment of the MM in alkalis, FeO and Al_2O_3 (Fig. 7), and silica (Fig. 8b). (2) The Fe/Mg ratio remains generally uniform for all analyses, with only a few exceptions of Fe-enrichment reflecting areas strongly enriched in modal amounts of opaque phases. A similar case can be made for Fe:Ti, as shown by the proportion of normative ilmenite:magnetite (Fig. 8c). (3) The proportion of normative An:Ab (Fig. 8a) indicates two general groupings that correspond to the composition and abundance of plagioclase (see below) in the samples (i.e. calcic plagioclase (An_{50-60}) and sodic plagioclase), and also the presence of matrix zeolites. (4) Enrichment of normative Or, especially for the mesostasis material, reflects the presence of K-feldspar (sanidine ?) closely associated with quartz. These analyses reflect the petrographic occurrence of the granophyres noted previously (Fig. 4). (5) As is apparent from Figures 7 and 8, very few of the analyses from this study correspond to the area for fresh North Mountain Basalt; thus, one or more processes have resulted in modification of the primary basalt chemistry.

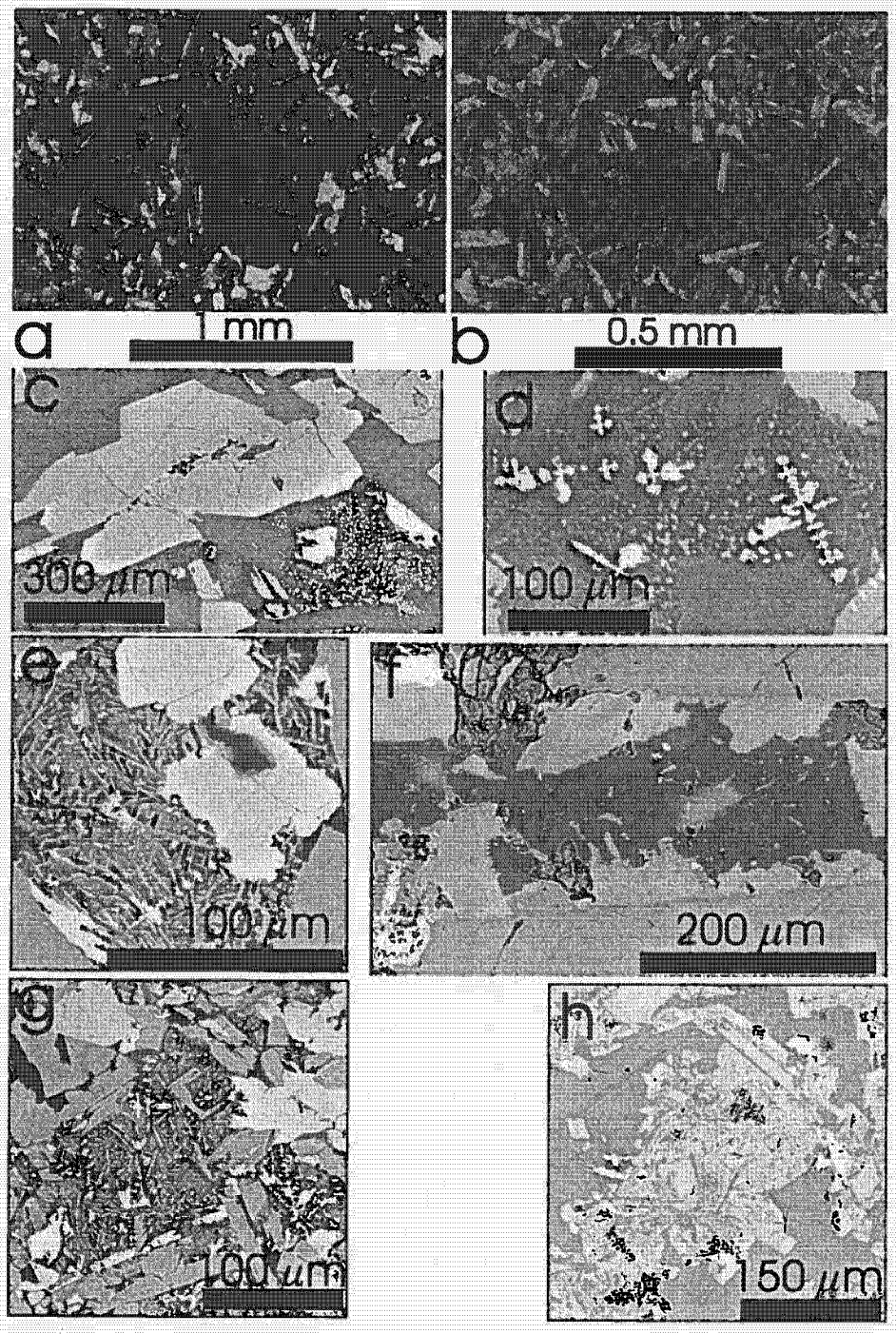

Figure 4. Petrographic features of the North Mountain Basalt, both massive and amygdaloidal. Pictures represent plane transmitted light (PTL) photos using petrographic microscope (Figs. a, b) and back-scattered electron images (BSE) taken with the electron microprobe (Figs. c to h). (a) Typical example of massive basalt with clinopyroxene and plagioclase crystals in finer grained matrix of similar mineralogy with addition of Fe-Ti oxide phase. Photo in crossed nicols. (b) Basalt with dark brown to black mesostasis material that is partially crystallized. This material represents original glass which may account for up to 25-30% of some basalt samples. Photo in PTL. (c) BSE image of clinopyroxene with an Fe-rich rim where in contact with the late-stage Fe-rich melt now full of micro-crystals of Fe-Ti oxide phase. (d) BSE image of skeletal Fe-Ti oxide phases in crystallized Fe-rich melt. (e) Late-stage Fe-rich melt with skeletal Fe-Ti oxides intergrown with spinifex textured crystallites. Note the small clinopyroxene grains with Fe-rich rims (bright border). (f) Feldspar overgrowths on large calcic plagioclase grain. Feldspar overgrowths are K-feldspar (Kf) and albitic plagioclase (Ab). (g) Similar to e. (h) Granophyre which formed from crystallization of late-stage felsic melt.

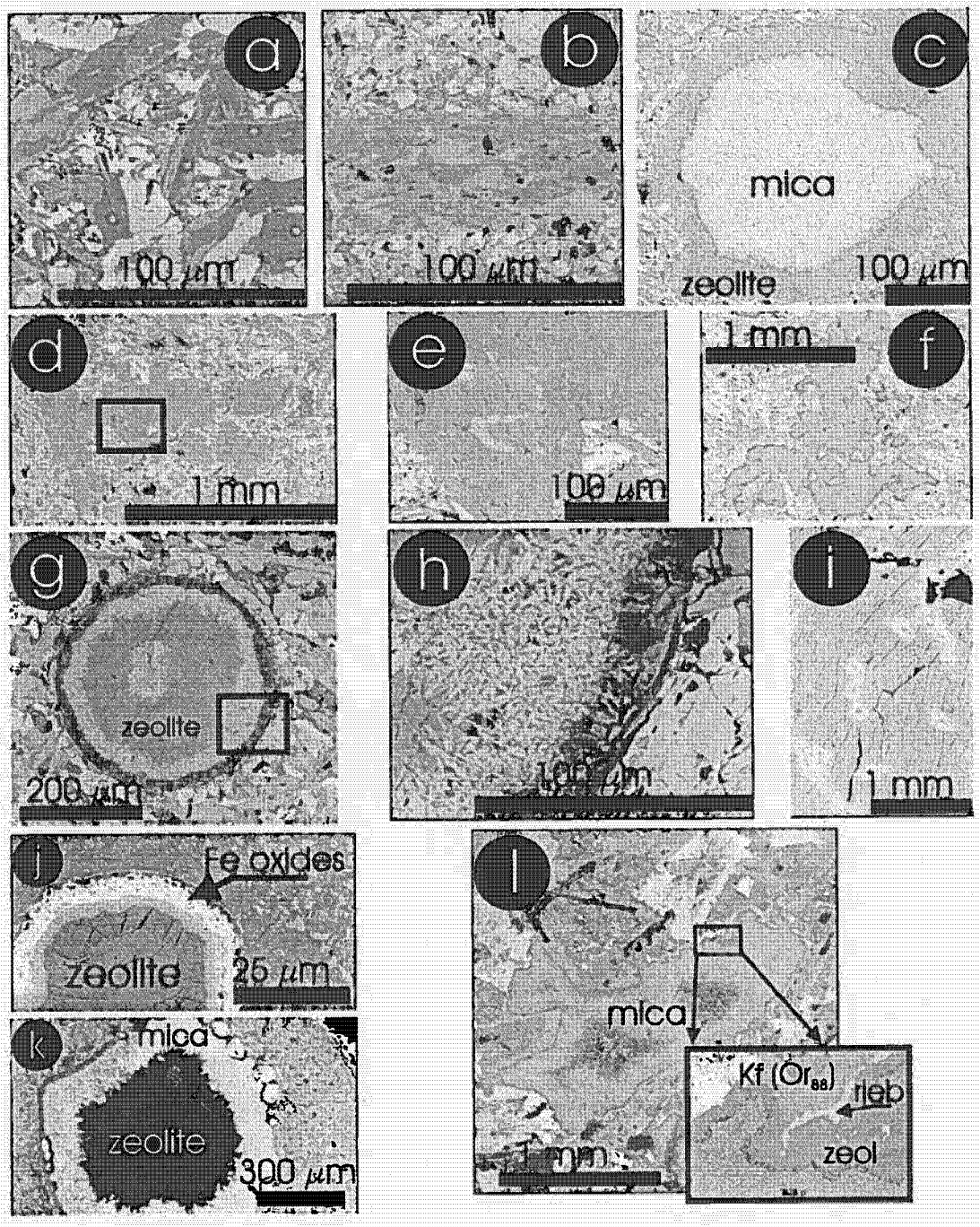

Figure 5. Back-scattered electron (BSE) images of secondary mineralogy in basalt, including amygdule phases. (a) Basalt showing albitization of the plagioclase as noted by the dark phase in the middle of the plagioclase grains. Note how fresh the pyroxene has remained. (b) Close-up of an albitized and zeolitized plagioclase with remnant patches of calcic plagioclase preserved. (c) Mica phase coring zeolite amygdule. (d, e) Zeolite pseudomorphing plagioclase and cut by later K-feldspar phase. Box in Figure 5d indicates area enlarged in Figure 5e. (f) Very irregular shaped amygdule characteristic of the finer grained amygdules in basalt. The dark rim is biotite phase and core is zeolite. (g,h) Spherical amygdule rimmed by varied mica phases and cored by zeolite. Note the box in Figure 5g is enlarged in Figure 5h and shows the delicate fibrous nature of the micas. Note how fresh the pyroxene is adjacent to the amygdule. (i) Zeolite in amygdule replaced by later mica phases. (j) Amygdule rimmed by Fe oxide phases and cored by zeolite. (k) Amygdule infilled by micas and zeolite. The bright spheres are various Fe-oxide phases. (l) Irregular shaped amygdule with rim of K-feldspar which is followed by zeolite and finally mica, but with a thin vein of alkali amphibole (riebeckite; rieb).

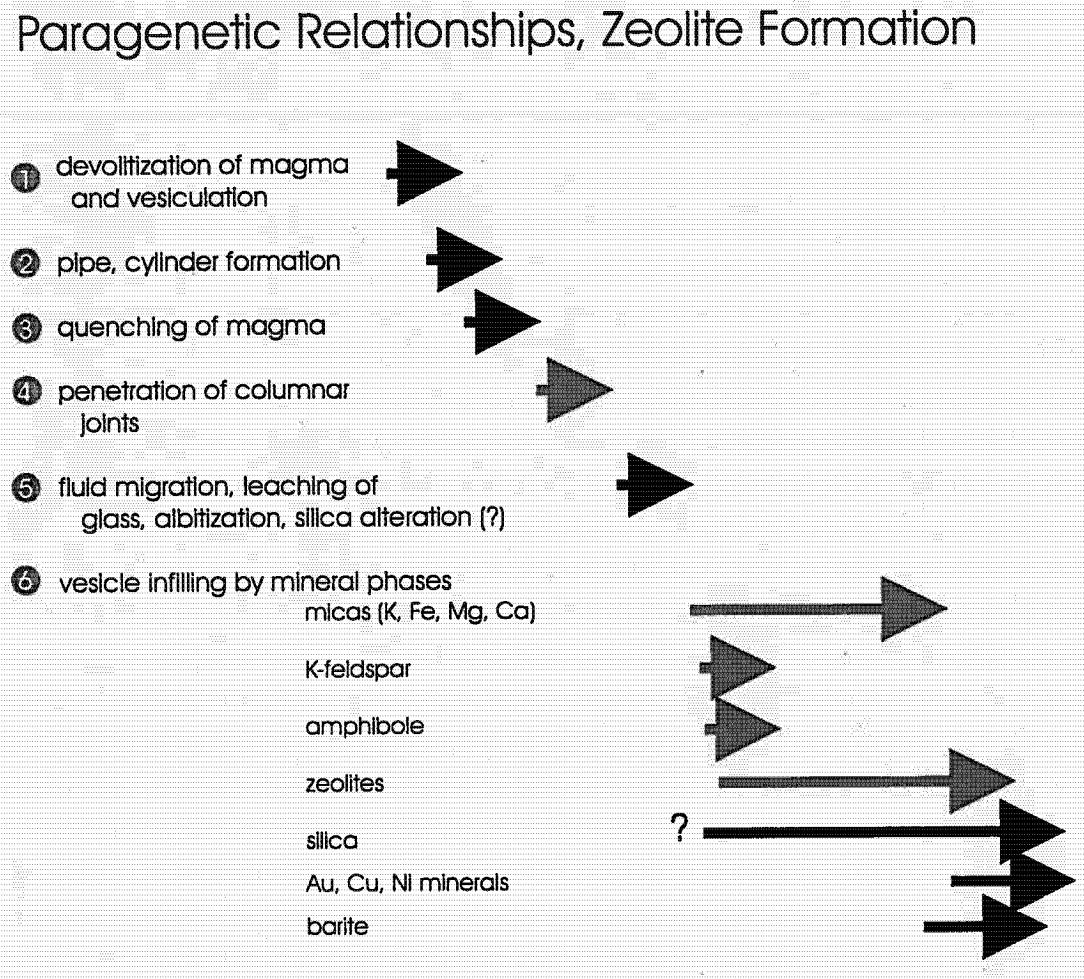

Figure 6. Paragenesis for the North Mountain Basalt containing zeolites and other amygdule phases, including the barite and Au, Cu and Ni mineralization of Pe-Piper (1997).

Mineral Chemistry

Mineral chemistry has been obtained for both primary (pyroxene, plagioclase, oxides) and secondary (zeolite, mica, feldspar, amphibole) phases and these are discussed separately below.

Pyroxene compositions are plotted in the standard pyroxene quadralateral in Figure 9 and are compared in this diagram to results from Greenough and Dostal (1992b, c) and to the trend for the Skaergaard intrusion. Pyroxene samples correspond to the following groups. (1) Augitic pyroxene is the most common of the phenocrystic pyroxenes, and is normally zoned from an Mg-rich core to an Fe-rich rim. A single matrix pyroxene falls at the Fe-rich end of this field. (2) Ferroaugite is restricted to narrow rims on augitic phenocrysts, as seen in back-scattered images (Fig. 4c, e). A single matrix pyroxene also falls in this field. (3) Pigeonitic pyroxene falls in the range below subcalcic augite, which has the same broad range in terms of Fe:Mg as the augite-ferroaugite. Again, a single matrix pyroxene falls in this field. (4) Two analyses correspond to orthopyroxene of En_{40-20} composition. Analytical data from apparently altered pyroxene (i.e. red-brown material coring grains) generally overlap the field for fresh pyroxene (Fig. 9). In general, the pyroxene compositions compare well with previous mineral chemistry data for this mineral reported by Dostal and Greenough (1992b, c), although it is noted that their extreme Fe-rich compositions are for pyroxene hosted by mafic pegmatite and rhyolite within the basalt flows, and follow the crystallization trend for the Skaergaard intrusion.

Feldspar compositions, plotted in the An-Ab-Or ternary diagram in Figure 10, can be subdivided into the following compositional groups. (1) Calcic plagioclase of An_{50-70} composition occurs in phenocrystic and matrix grains. (2) Sodic plagioclase occurs as phenocrystic grains of An_{10-20} composition and matrix grains which are albitic (An_{0-10}), and include grains that are either

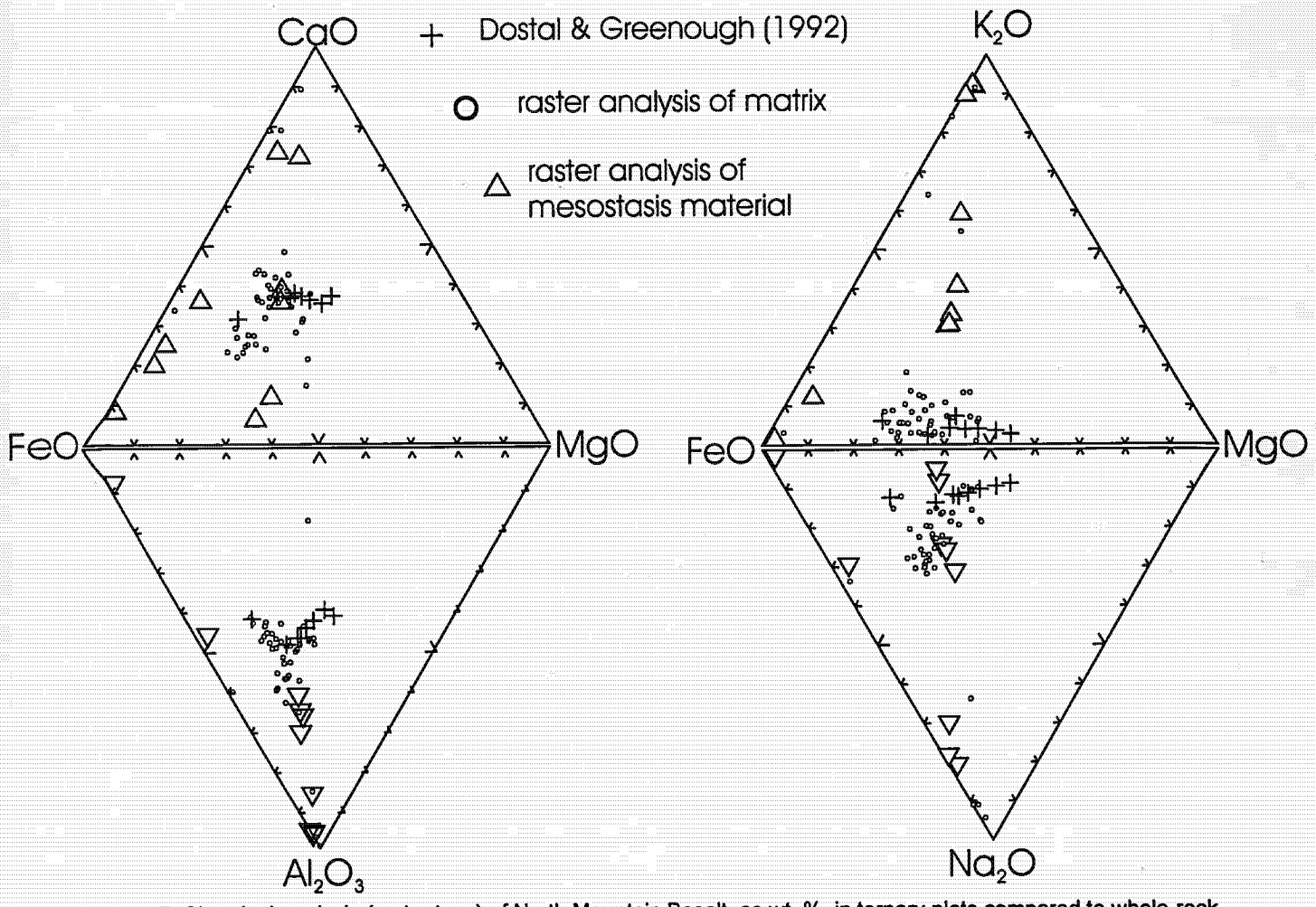

Figure 7. Chemical analysis (raster type) of North Mountain Basalt, as wt. %, in ternary plots compared to whole-rock compositions of similar material from Greenough and Dostal (1992a). The chemical data are subdivided into matrix analysis and intergranular matrix (originally glass material).

partially or totally replaced by albite. (3) Potassic feldspar of $Or_{90\text{-}100}$ composition occurs as intergrowths within intergranular material (i.e. originally glass), lining vesicles in amygdaloidal basalt (Fig. 5l) and as micro-veinlets and blebs cross-cutting and replacing zeolitized plagioclase (Fig. 5d, e). (4) Ternary feldspar of ca. $An_{10}Ab_{50}Or_{40}$ composition occurs as intergranular material (i.e. originally glass).

The oxide phases are mixed Fe-Ti minerals whose composition appears from preliminary work to be texture dependent. The equant grains are not magnetite, as expected where immiscible Fe-rich melts form (Philpotts, 1982); instead the mixed Fe-Ti compositions approximating ilmenite chemistry reflect the reduced nature of the melts. Further work is in progress with respect to oxide mineralogy.

Zeolite chemistry, which is dominated by Si, Al, Ca, Na and K and structural water, is summarized in ternary plots of cationic proportions in Figure 11, where the results are compared to stoichiometric end-member compositions of zeolites using mineral formulae in Deer *et al.* (1962). The chemical data have been subdivided into the three types of zeolite occurrences, namely: (1) infilling vugs or amygdules, (2) replacing phenocrystic or matrix plagioclase, and (3) within the matrix. There is a clear compositional variation for the zeolites, but within a single grain the chemistry is generally uniform, that is to say that variation may occur within the scale of a thin section rather than a grain. The compositions determined correspond to a large variety of zeolite minerals and based solely on their composition it is not possible to discriminate among the various types. Instead it is necessary to integrate the chemical data with field observations and X-ray diffractometry (XRD) work, of which the latter remains to be done. Other workers (e.g. Birch, 1989; Pe-Piper, 1997) have noted similar difficulty in distinguishing among zeolites based on chemical analysis. At present, based on the Si:

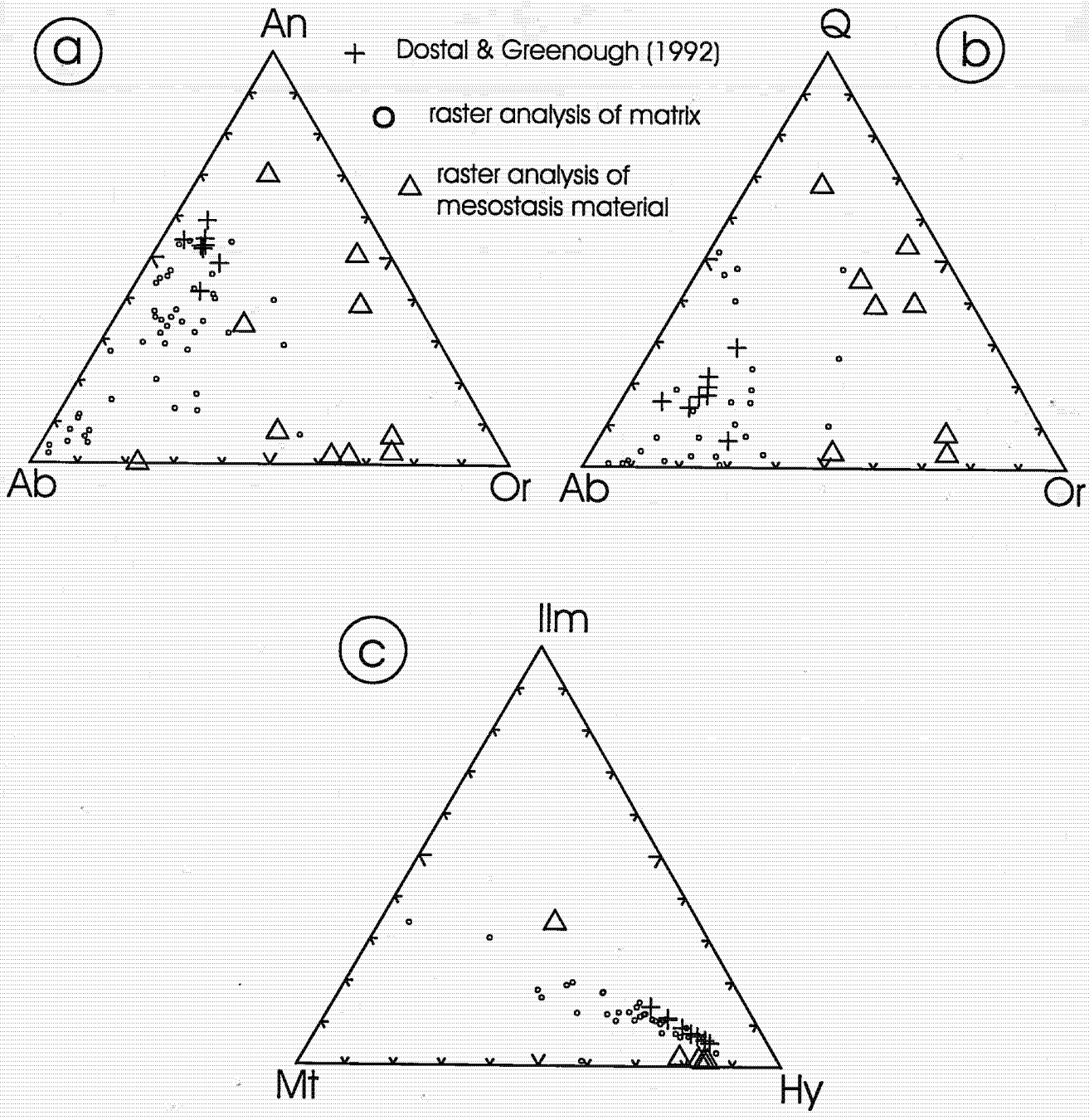

Figure 8. Chemical analysis (raster type) of North Mountain Basalt, as normative compositions, in ternary plots compared to whole-rock compositions of similar material from Greenough and Dostal (1992a). The chemical data are subdivided into matrix analysis and mesostasis material (originally glass material).

Al and Ca:Na ratios, which appear to be the best discriminators, the data are interpreted to indicate that the dominant zeolites are mainly heulandite, mordenite, chabazite and stilbite, with minor epistilbite, laumontite and thomsonite. The largest chemical variation is for zeolite infilling vugs, whereas the chemistry of zeolites replacing plagioclase and occurring in the matrix is relatively restricted.

The mica chemistry is highly variable, as summarized in various ternary and binary plots in Figure 12, and it is emphasized that these micas occur in close association. Note that in these diagrams a separation of data was arbitrarily chosen at 2 wt. % CaO in order to separate the data into what may possibly be different mica types. In the standard Al-Fe+Mg-Si ternary and Al (total) and Fe+Mg binary plots, the

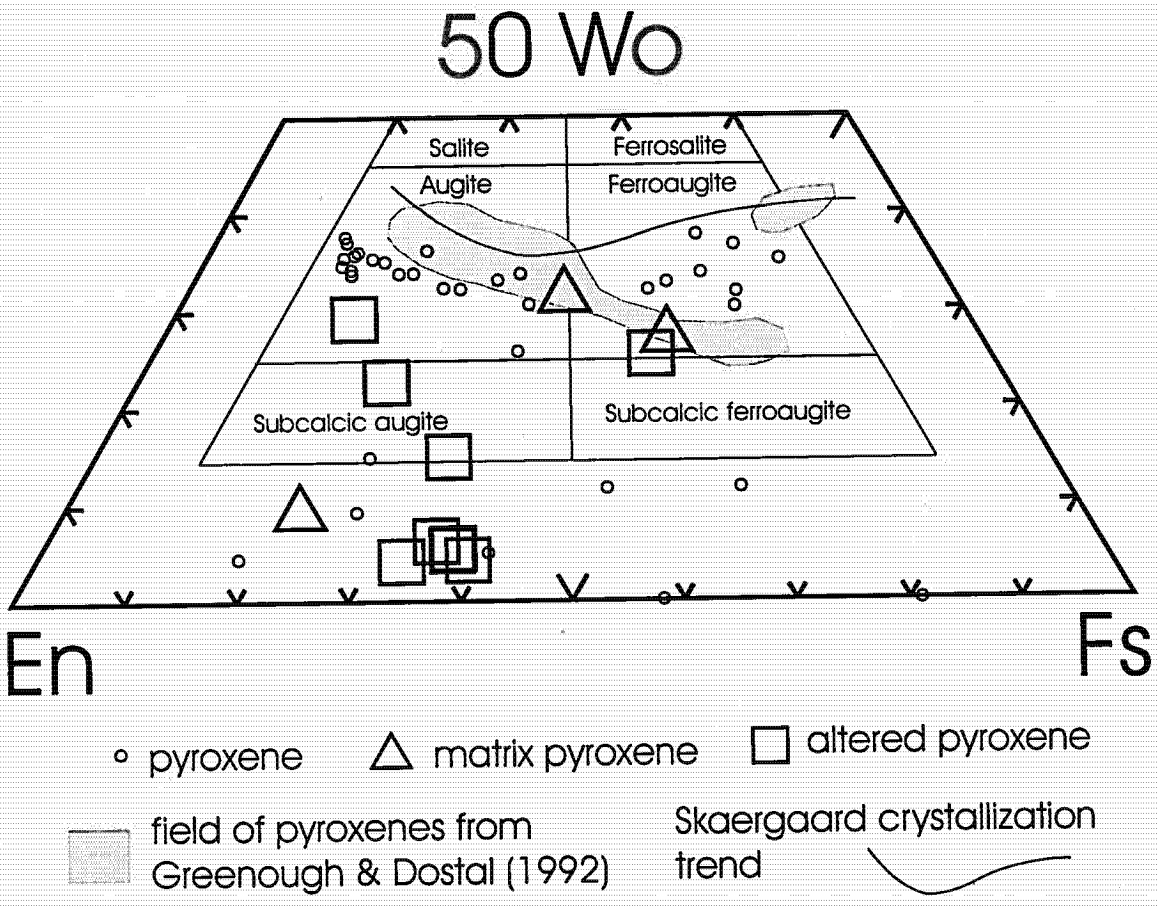

Figure 9. Pyroxene compositions plotted in the partial Ca-Mg-Fe quadralateral (50Wo-En-Fs) with pyroxene classification after Deer *et al.* (1962). The field for pyroxene compositions in the North Mountain Basalt from Greenough and Dostal (1992b,c) and Skaergaard crystallization trend are shown for comparison.

majority of data forms a continuum from muscovite to leucophyllite/celadontite. A few analyses with the most enrichment in Fe+Mg plot close to the biotite/annite Al-Fe+Mg-Si ternary. A large range in wt. % K_2O is apparent in Figure 12d, with two trends apparent: one an exchange with CaO toward margarite or clintonite/ xenophyllite, and the other possibly related to chloritization, since neither substantial K or Ca is present in these micas. A positive correlation occurs for wt. % Na_2O and CaO (Fig. 12c), which together may account for 15 wt.% of the analysis. A substitution towards margarite/clintonite is suggested in Figures 12b and 12f. Clearly, additional work is required to further refine the nature of the mica phases.

A single occurrence of alkali amphibole was noted in one sample where it occurred along with K-feldspar (Fig. 5l). The chemical analysis of this mineral (Table 1) is similar to the alkali amphiboles arfvedsonite and riebeckite, as given in Deer *et al.* (1962), but the North Mountain Basalt sample is slightly higher in calcium. Using the classification scheme of Hawthorne (1981), the sample also corresponds to these two amphiboles, although the high sodic content would favour classification as arfvedsonite.

Discussion

Zeolites in the North Mountain Basalt occur in several distinct zones within individual flows that can be traced laterally for considerable distances. Formation of these zones reflects two separate phenomena: first, distribution of gas within flows and second, infiltration of a hydrothermal fluid which was responsible for precipitation of the zeolites and related phases. In the following discussion the distribution of zeolites is first addressed, followed by a discussion of their nature and origin.

Table 1. Composition and structural formulae for an amphilbole gain in amygdule, North Mountain Basalt (two analyses).

Component	Analysis 1 (%)	Analysis 2 (%)
SiO_2	49.25	49.93
TiO_2	0.06	0.09
Al_2O_3	0.58	0.16
FeO	28.21	29.90
MnO	0.45	0.47
MgO	1.53	0.60
CaO	5.28	3.19
Na_2O	10.37	11.75
K_2O	ND	ND
P_2O_5	ND	ND
BaO	ND	ND
Total	95.82	96.20
Structural formulae based on 23 oxygen (Fe as Fe^{2+})		
Si	8.000	8.112
Ti	0.007	0.011
Al	0.111	0.030
Fe	3.832	4.067
Mn	0.061	0.064
Mg	0.370	0.145
Ca	0.919	0.556
Na	3.266	3.706

Distribution of Vesicles and Mechanism of Formation

The distribution of vesicles (amygdules prior to infilling) in the North Mountain Basalt can be interpreted in the context of vesicles in basalt flows based on natural observations and combined experimental and modelling work, as summarized in Figure 13a. Vesicle distribution in the North Mountain Basalt (Fig. 3) is summarized schematically in Figure 13b and compared to distribution in other flows in Figure 13a. The comparison is striking and similar mechanisms of formation are suggested given that the host rocks are similar, being continental flood basalts of tholeiitic composition with pahoehoe features. Formation of the different zones of vesicles is summarized below, as described by Walker (1987), Goff (1996), Manga and Stone (1994) and Manga (1996), among others.

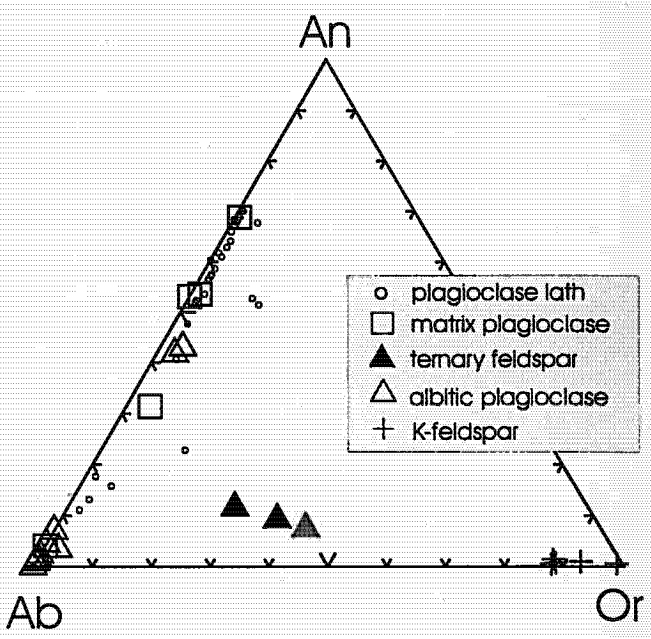

Figure 10. Feldspar compositions in An-Ab-Or ternary plot. Note that the ternary feldspar occurs in the inter-granular matrix (i.e. original glass material) and K-feldspar (Or_{90-100}) as veins cutting zeolite.

Erupting basaltic magma contains a certain initial quantity of gas formed from bubble nucleation during ascent and eruption, as represented by the uppermost frothy flow-top zone in flows (Walker, 1987). Many factors control the abundance of such bubbles, including atmospheric pressure; thus, considerable variation might be expected in the abundance of vesicles and this is what is often observed. The bottom zone, containing pipe vesicles and randomly distributed vesicles between pipes, reflects the buoyant rise of gas bubbles, with the gas either of external or internal origin. The external reservoir may be represented by water derived from an underlying reservoir overridden by the lava flows (e.g. small streams, puddles, etc.), whereas the internal reservoir is the crystallizing basaltic magma which liberates dissolved gases (H_2O, CO_2; e.g. Bottinga and Javoy, 1991). The actual formation of the pipes remains controversial (e.g. Walker, 1987; Philpotts and Lewis, 1997) and is not addressed here. The fact that most of

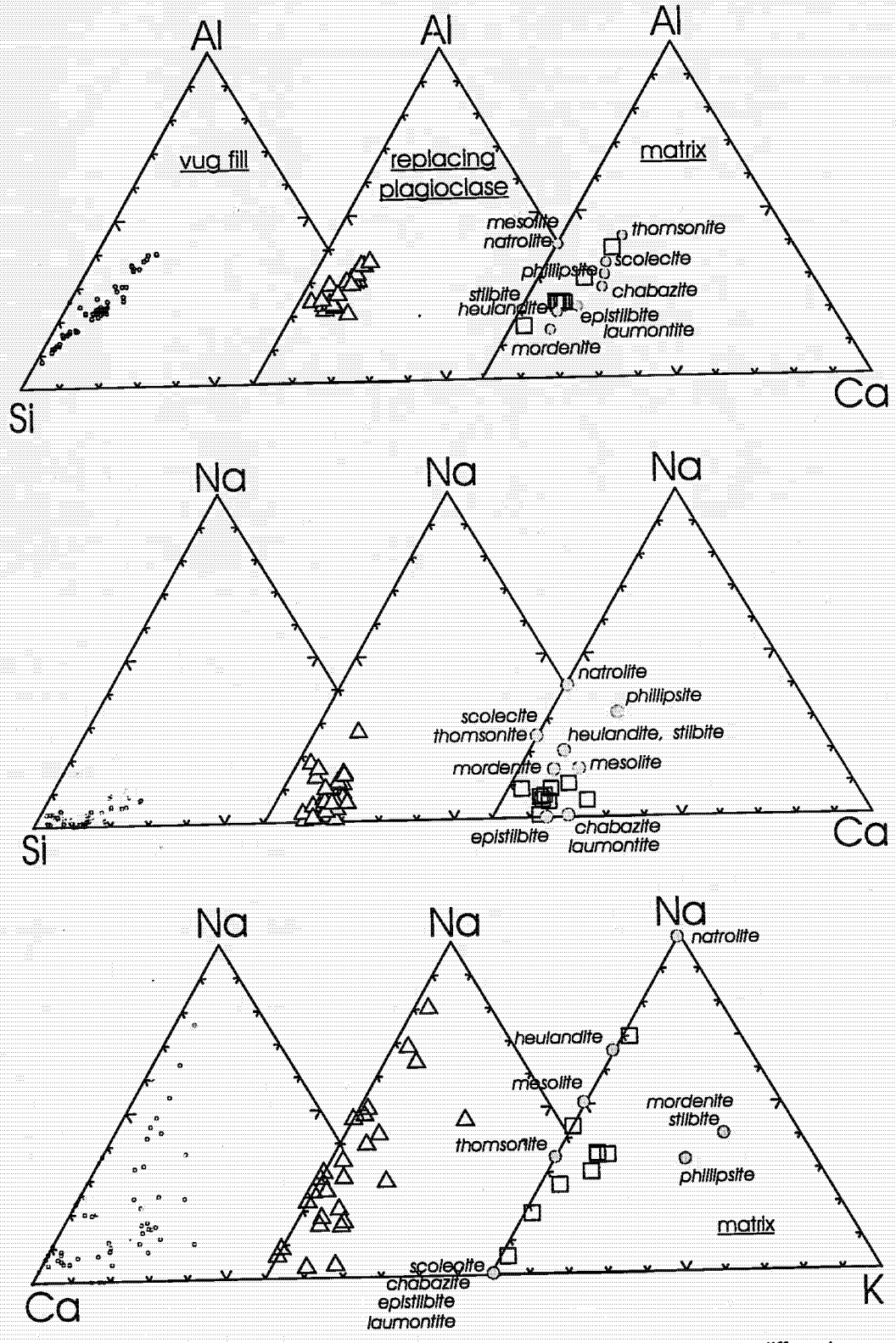

Figure 11. Ternary plots of zeolite analyses as cationic proportions plotted in terms of three different occurrences of zeolites, namely infilling vugs, replacing feldspar and within the matrix. The end member compositions for different zeolites are from Deer *et al.* (1962).

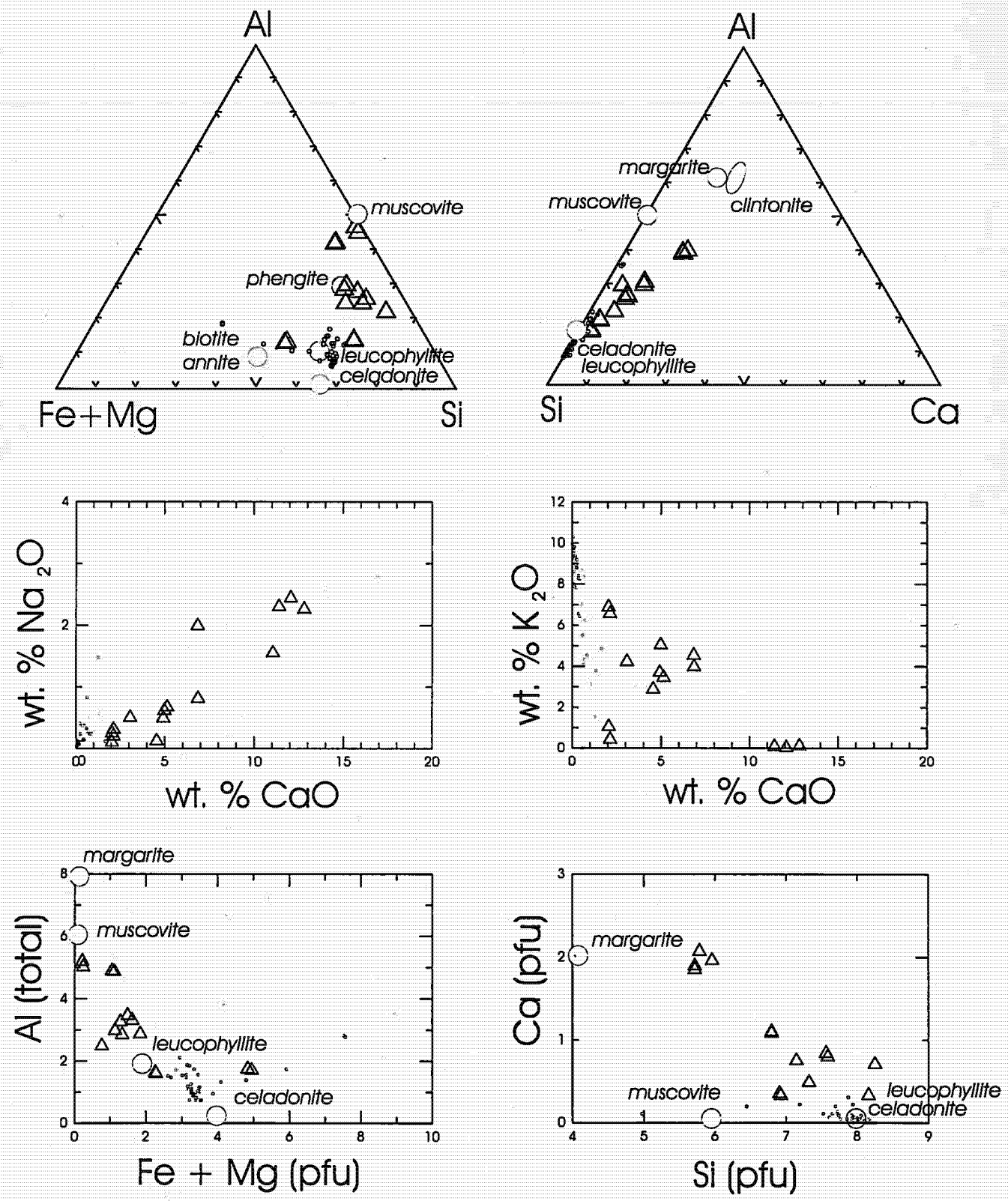

Figure 12. Chemical analysis of muscovite in ternary and binary plots based on 22 oxygen. (a) Ternary Al-Fe+Mg-Si plot (cationic proportions). (b) Ternary Al-Si-Ca plot (cationic proportions). (c) Binary element plot of wt. % Na_2O versus wt. % CaO. (d) Binary element plot of wt. % K_2O versus wt. % CaO. (e) Binary plot of Al (total) versus Fe+Mg (per formula unit). (f) Binary plot of Ca versus Si (per formula unit). End-member compositions for different micas are based on formulae in Deer *et al.* (1962).

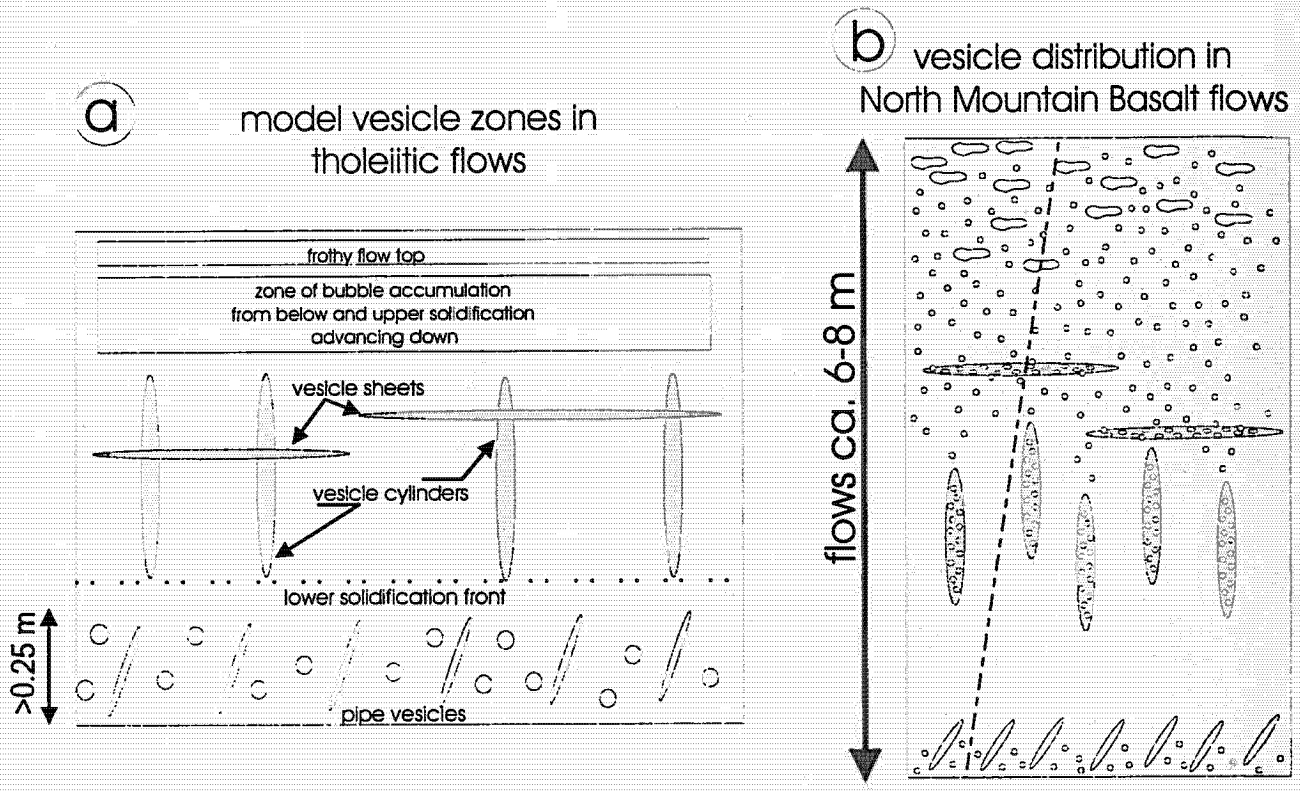

Figure 13. Comparison of the distribution of vesicles/amygdules in a model tholeiitic flow (McMillan *et al.*, 1987; Walker, 1987; Manga and Stone, 1994; Goff, 1996; Manga, 1996) and those observed in the flows of the North Mountain Basalt.

the pipes are inclined indicates that pipe formation preceded complete cessation of flow movement and solidification of the basalt within the bottom 1 m, which contrasts with the vertical alignment of the vesicle cylinders in the centres of flows. This observation implies a difference in timing for formation of vesicles between the two zones. Vesicle cylinders occur within the central zone and vesicle sheets merge vertically into the network zone. Their formation reflects the movement of internally generated gas into buoyant plumes and relates to the combined effects of gravitational instability and bubble coalescence and migration. Bubbles are generated due to solidification of the basaltic magma (i.e. lower solidification front) which forms a bubble-rich layer that subsequently becomes unstable in the dense basaltic liquid and begins to behave buoyantly. Although the exact model by which this mechanism operates remains uncertain (Manga and Stone, 1994; Goff, 1996), the process is generally accepted and supported by the exceptional examples preserved in places like the Columbia River basalts (McMillan *et al.*, 1987, 1989), the features of which have been successfully modelled by Manga (1996). Within the North Mountain Basalt, it should be noted that, as elsewhere (Goff, 1996), the lower bubble zone generated above the lower solidification front is not preserved within the flows, for a reason which remains unresolved.

Although not addressed or noted in other studies of vesiculated basalts, the presence of planar sheets of amygdules in the flow tops (Fig. 3g) deserves comment. This feature is locally dominant and may reflect the presence of an upper solidification front (McMillan *et al.*, 1987; Aubele *et al.*, 1988) but which is generally developed at a greater distance from the flow-top zone than observed in the case of the North Mountain Basalt. One possible explanation for the proximity of the zone to the flow top in the North Mountain Basalt is that part of the overlying basalt was eroded prior to deposition of the overlying flow, hence removing the existing evidence of the flow-top zone. Further work will be devoted to resolving this apparently unusual feature.

In summary, the different zones of vesicles in the North Mountain Basalt are similar to those documented in continental tholeiitic basalts elsewhere and their origin can be related to vesiculation of the basalts as they erupt and later crystallize. The bubbles reflect effervescence of volatiles (H_2O, CO_2) of both internal

and external origin, with the latter relating to the formation of pipe vesicles in flow bottoms.

Origin of Amygdules

Infilling of the vesicles in the North Mountain Basalt required infiltration of a fluid after solidification of the basalt flows. In addition, the range of mineral phases comprising the amygdules and their compositional diversity (e.g. micas) predicate considerable variability and/or fluctuation in fluid composition. Given that the vesicles are infilled by a variety of Fe, Mg, Ca, Na, K, and Al silicates, both anhydrous and hydrous, and that there is considerable preservation of the primary silicate phases in the basalts, especially the pyroxenes, it is probable that the aforementioned elements were leached out of the mesostasis of the basalts. As noted earlier, there is considerable evidence that extensive, late-stage liquid immisicibility occurred in the North Mountain Basalt and their contrasting bulk compositions indicate a way of generating quite different fluid compositions, albeit on a local scale. In support of this scenario, it is relevant to emphasize that there is ample evidence from alteration studies of basaltic rocks, in particular ocean floor material studied in both the natural and experimental environment, to indicate that glass is readily leached by hot fluids. Thus, a model is proposed for zeolite formation in the North Mountain Basalt which first involves leaching of cations from pre-existing glass in the mesostasis of the basalt, and subsequent infilling of vesicles. The mineral zonation observed (e.g. Fig. 6) reflects both an evolving and changing fluid chemistry. In some cases there are subtle changes, as recorded by slight variation in the composition of mica or zeolite traversed with the electron microprobe, but in marked contrast to this is the abrupt change to a new mineralogy which occurs commonly.

Conditions of Amygdule Formation

The amygdule mineralogy provides some constraints on the temperature of formation, based on the known stability fields of the various minerals present. Pe-Piper (1997) notes that the presence of mordenite with labradorite suggests temperatures in excess of 250°C, whereas the occurrence of K-feldspar of Or_{90} composition overlapping zeolite deposition and locally coexisting with alkali amphibole suggests even higher temperatures of deposition (ca. 350°C). The mica phases present (rather than clay minerals such as kaolinite) also favour high temperatures, probably well in excess of 300°C (Hewitt and Wones, 1984). Further work, including fluid inclusion study and stable isotope analysis, is planned to further constrain the conditions of formation.

Summary, Conclusions and Future Work

Initial results of a study focused on zeolite distribution in basalt flows of the Jurassic North Mountain Basalt has established a four zone classification that is shown to be consistent within and between flows and is laterally continuous. Comparison to previous studies documenting the distribution of vesicles within similar quartz-normative, continental tholeiites with pahoehoe flow characteristics (e.g. Columbia River basalts) indicates a very similar vertical profile for vesicle types: a basal pipe-vesicle zone, a central cylinder- and sheet-vesicle zone, and an upper, frothy flow-top zone. The distribution of these vesicles is consistent with both experimental and theoretical studies that document formation and coalescence of bubbles within flows that result from both externally and internally derived gas components. For example, the pipe-vesicle dominated bottom zone reflects incursion of an external component early in the flow history resulting from the flow over-riding a water-rich horizon, in contrast to the central zone of cylinder- and sheet-vesicles that relate to a moving solidification front, and finally the frothy flow top which reflects the nucleation of bubbles during ascent and eruption. Preservation of this vesicle distribution reflects entrainment of gas pockets (bubbles) at the time when the flow solidified.

Subsequent infilling of the vesicles records the infiltration and circulation of an externally derived fluid, the nature of which remains to be defined. Leaching of elements from late-stage mesostasis glass, which records liquid immiscibility textures and compositions of both felsic and basic nature, provided the solutes that went into forming the amygdules. A clear paragenesis is present with the early stages dominated by Fe-, Mg- and Ca-rich potassium mica, followed by a zeolite-dominant stage. Future work will focus on constraining the thermal conditions of these stages.

The important findings of the present study may be summarized in the following points. (1) Correlation of the amygdule-rich zones with a well-documented distribution of such zones in basalt flows provides a consistent means of following these zones in three dimensions, which is of relevance to exploration and development of the zeolites. (2) The occurrence of zeolites within the non-vesiculated part of the flows is documented for the first time. This information is

relevant because these matrix zeolites may account for a large percentage of the cation exchange capacity of a rock and must be considered when assessing the economic potential of zeolite-bearing rocks. In addition, since such material is not visibly enriched in zeolites, it might be overlooked in terms of its potential for economic application. This observation also accounts for the anomalously high cation exchange capacity values (CECs) obtained for whole-rock material of North Mountain Basalt (G. A. O'Reilly, personal communication, 1999).

References

Anderson, A. T., Jr., Swthart, G. H., Artioli, G. and Geiger, C. A. 1984: Segregation vesicles, gas filter-pressing and igneous differentiation; Journal of Geology, v. 92, p. 55-72.

Aubele, J. C., Crumpler, L. S. and Elston, W. E. 1988: Vesicle zonation and vertical structure of basalt flows; Journal of Volcanolgy and Geothermal Research, v. 35, p. 349-374.

Aumento, F. 1962: An X-ray study of some Nova Scotia zeolites; unpublished M.Sc. thesis, Dalhousie University, Halifax, Nova Scotia, 104 p.

Birch, W. D. (editor) 1989: Zeolites of Victoria; The Mineralogical Society of Victoria, Inc., Glove Press Pty. Ltd., Australia, 110 p.

Bottinga, Y. and Javoy, M. 1991: The degassing of Hawaiian tholeiite; Bulletin of Volcanology, v. 53, p. 73-85.

Colwell, J. A. 1980: Zeolites in the North Mountain Basalt, Nova Scotia; Geological Association of Canada-Mineralogical Association of Canada, Annual Meeting, Field Guidebook, 16 p.

Deer, W. A., Howie, R. A. and Zussman, J. 1962: An Introduction to the Rock-forming Minerals; Longman Group Ltd., London, 528 p.

Goff, F. 1996: Vescicle cylinders in vapor-differentiated basalt flows; Journal of Volcanology and Geothermal Research, v. 71, p. 167-185.

Greenough, J. D. and Dostal, J. 1992a: Geochemistry and petrogenesis of the early Mesozoic North Mountain Basalt of Nova Scotia, Canada; *in* Eastern North American Mesozoic Magmatism, eds. J. H. Puffer and P. C. Ragland; Geological Society of America, Special Paper 268, p. 149-159.

Greenough, J. D. and Dostal, J. 1992b: Cooling history and differentiation of a thick North Mountain Basalt flow (Nova Scotia, Canada); Bulletin of Volcanology and Geothermal Research, v. 55, p. 63-73.

Greenough, J. D. and Dostal, J. 1992c: Layered rhyolite bands in a thick North Mountain Basalt flow: the products of silicate liquid immiscibility; Mineralogical Magazine, v. 56, p. 309-318.

Greenough, J. D. and Papezik, V. S. 1987: Note on the petrology of the North Mountain Basalt from the wildcat oil well Mobil Gulf Chinampas N-37, Bay of Fundy, Canada; Canadian Journal of Earth Sciences, v. 24, p. 1255-1260.

Greenough, J. D., Jones, L. M. and Mossman, D. J. 1989: Petrochemical and stratigraphic aspects of North Mountain Basalt from the north shore of the Bay of Fundy, Nova Scotia, Canada; Canadian Journal of Earth Sciences, v. 26, p. 2710-2717.

Hawthorne, F. C. 1981: Crystal chemistry of the amphiboles; *in* Amphiboles and Other Hydrous Pyriboles, ed. D. R. Veblen; Mineralogical Society of America, Reviews in Mineralogy, v. 9A, p. 1-102.

Hewitt, D. A. and Wones, D. R. 1984: Experimental phase relations of the micas; *in* Micas, ed. S. W. Bailey; Mineralogical Society of America, Reviews in Mineralogy, v. 13, p. 210-256.

Hodych, J. P. and Dunning, G. R. 1992: Did the Manicouagan impact trigger end-of-Triassic mass extinction?; Geology, v. 20, p. 51-54.

Hudgins, A. D. 1960: The geology of the North Mountain in the map area, Baxters Harbour to Victoria Beach; unpublished M.Sc. thesis, Acadia University, Wolfville, Nova Scotia.

Manga, M. 1996: Waves of bubbles in basaltic magmas and lavas; Journal Geophysical Research, v. 101, p. 17,457-17,465.

Manga, M. and Stone, H. A. 1994: Interactions between bubbles in magmas and lavas: effects of bubble deformation; Journal of Volcanology and Geothermal Research, v. 63, p. 267-279.

Mangan, M. T., Cashman, K. V. and Newman, S. 1993: Vesiculation of basaltic magma during eruption; Geology, v. 21, p. 157-160.

Marshall, S. 1999: North Mountain zeolite deposits (abstract); Atlantic Geology, v. 35, p. 97.

McMillan, K., Cross, R. W. and Long, P. E. 1987: Two-stage vesiculation in the Cohassett flow of the Grande Ronde Basalt, south-central Washington; Geology, v. 15, p. 809-812.

McMillan, K., Long, P. E. and Cross, R. C. 1989: Vesiculation in Columbia River basals; *in* Volcanism and Tectonism in the Columbia River Flood-Basalt Province, eds. S. R. Reidel and P. R. Hooper; Geological Society of America, Special Paper 239, p. 157-167.

Papezik, V. S., Greenough, J. D., Colwell, J. A. and Mallinson, T. J. 1988: North Mountain basalt from Digby, Nova Scotia: models for fissure eruption from stratigraphy and petrochemistry; Canadian Journal of Earth Sciences, v. 25, p. 74-83.

Pe-Piper, G. 1997: Origin of zeolites in zoned amygdales from the North Mountain Basalt, Nova Scotia; Atlantic Geology, v. 33, p. 74.

Pe-Piper, G. and Horton, D. 1996: Zeolite mineral assemblages in the North Mountain Basalt, Nova Scotia; Nova Scotia Department Natural Resources, Open File Report 96-001, 30 p.

Philpotts, A. R. 1978: Textural evidence for liquid immiscibility in tholeiites; Mineralogical Magazine, v. 324, p. 417-425.

Philpotts, A. R. 1979: Silicate liquid immiscibility in tholeiitic basalts; Journal of Petrology, v. 20, p. 99-118.

Philpotts, A. R. 1982: Compositions of immiscible liquids in volcanic rocks; Contributions to Mineralogy and Petrology, v. 80, p. 201-218.

Philpotts, A. R. and Lewis, C. L. 1987: Pipe vesicles - An alternate model for their origin; Geology, v. 15, p. 971-974.

Sahagian, D. 1985: Bubble migration and coalescence during the solidification of basaltic lava flows; Journal of Geology, v. 93, p. 205-211.

Walker, G. P. 1987: Pipe vesicles in Hawaiian basaltic lavas: their origin and potential as paleoslope indicators; Geology, v. 15, p. 84-87.

C1085-020